Redox Biology 20 (2019) 195–203

Contents lists available at ScienceDirect

Redox Biology

journal homepage: www.elsevier.com/locate/redox

Research Paper

# Efficacy of 5-aminolevulinic acid–based photodynamic therapy against keloid compromised by downregulation of SIRT1-SIRT3-SOD2-mROS dependent autophagy pathway

Tao Liu[1], Xiaorong Ma[1], Tianxiang Ouyang*, Huiping Chen, Yan Xiao, Yingying Huang, Jun Liu, Miao Xu

*Department of Plastic and Reconstructive Surgery, Xinhua Hospital, School of Medicine, Shanghai Jiao Tong University, People's Republic of China*

ARTICLE INFO

*Keywords:*
Keloid
5-aminolevulinic acid
SIRT1
SIRT3
Autophagy

ABSTRACT

Keloids exhibit cancer-like properties without spontaneous regression and usually recur post excision. Although photodynamic therapy (PDT) is a promising treatment, details of the mechanisms remain to be elucidated. In this study, we investigated mechanisms involved in 5-Aminolevulinic Acid (5-ALA)–based PDT against keloid. Found that 5-ALA-PDT induced superoxide anion-dependent autophagic cell death. Application of autophagy inhibitor 3-Methyladenine (3-MA) significantly prevented the effect that 5-ALA-PDT induced keloid–derived fibroblasts death, but Z-VAK-FMK (apoptotic inhibitor) did not. Interestingly, 5-ALA-PDT promoted the SIRT3 protein expression and the activity of mitochondrial superoxide dismutase 2 (SOD2), but SIRT1 protein expression level was decreased. SOD2 as a key enzyme can decrease mitochondrial ROS (mROS) level, Deacetylation of SOD2 by SIRT3 regulates SOD2 enzymatic activity has been identified. Then we explored SOD2 acetylation level with immunoprecipitation, found that 5-ALA-PDT significantly increased the acetylation levels of SOD2. In order to confirm deacetylation of SOD2 regulated by SIRT3, 3-TYP (SIRT3 inhibitor) was used. Found that inhibition of SIRT3 by 3-TYP significantly increased the level of SOD2 acetylation level compared with control group or 5-ALA-PDT group. To explore the connection of SIRT1 and SIRT3, cells were treated with EX527(SIRT1 inhibitor) or SRT1720 (SIRT1 activator), and EX527 increased SIRT3 protein level, however, SRT1720 displayed the opposite effect in the present or absence of 5-ALA-PDT. Moreover SIRT1-inhibited cells are more resistant to 5-ALA-PDT and showing decreased ROS accumulation. These results may demonstrate that 5-ALA-PDT induced SIRT1 protein level decreased, which promoted the effect of SIRT3 increased activity of SOD2 that can reduce mROS level, and then compromised 5-ALA-PDT induced autophagic cell death.

## 1. Introduction

Keloids are pathological scars characterized by an excessive proliferation of fibroblasts, abnormal deposition of collagen fibers, and inflammation, which exhibit cancer-like properties without spontaneous regression and usually recur post excision [1,2]. There are many forms of treatment for keloid, concerns regarding their low efficacy, side effects, and high risk of palindromia are frustrating challenges for surgeons. Hence, the search for safer and more effective therapies for keloid seems to be required urgently.

In recent years, PDT, an effective therapeutic approach with great spatiotemporal accuracy and minimal invasiveness, has aroused tremendous interests in keloid therapy [3,4]. The therapeutic procedure consists of three essential elements: a photosensitizer (5-ALA), laser irradiation, and production of reactive oxygen species (ROS). 5-ALA, a precursor of heme biosynthesis, when permeated in mitochondria, could be enzymatically converted into protoporphyrin IX, which in turn interacts with laser to produce ROS that ultimately trigger cell death [5]. 5-ALA-derived protoporphyrin IX exhibits rapid clearance from tissues [6]. Besides, phototoxicity was not displayed in cells treated

*Abbreviations:* NAD, nicotinamide adenine dinucleotide; ROS, reactive oxygen species; FBS, fetal bovine serum; SIRT1, sirtuin 1; SIRT3, sirtuin 3; mROS, mitochondrial reactive oxygen species; SOD2, superoxide dismutase 2, mitochondrial; PDT, photodynamic therapy; IP, immunoprecipitation; 5-ALA, 5-aminolevulinic acid; SQSTM1/p62, sequestosome 1; 3-MA, 3-methyladenine; 3-TYP, 3-(1H-1,2,3-triazol-4-yl)pyridine

* Correspondence to: Department of Plastic and Reconstructive Surgery, Xinhua Hospital, School of Medicine, Shanghai Jiao Tong University, No. 1665, kongjiang Road, Yangpu District, Shanghai, People's Republic of China.

*E-mail addresses:* lvnff@sina.cn, ouyangtianxiang@xinhuamed.com.cn (T. Ouyang).

[1] The first two authors are contributed equally to this article.

https://doi.org/10.1016/j.redox.2018.10.011
Received 3 September 2018; Received in revised form 9 October 2018; Accepted 15 October 2018
Available online 17 October 2018

with 5-ALA in the absence of irradiation [7]. Thus, the side effects of 5-ALA-PDT on normal tissues may be avoided with topical 5-ALA administration and well-directed laser irradiation.

Many studies have investigated the mechanisms Involved in 5-ALA-PDT, but these findings almost highlight the role of apoptosis in 5-ALA-PDT [4,7]. However, our previous assays demonstrated that apoptotic inhibitor did not prevent 5-ALA-PDT induced cells death. Herein the molecular mechanisms involved in 5-ALA against keloid remain to be elucidated. There is already growing evidence that excess autophagy may induce mitochondrial loss, cellular energy depletion and cell death [8,9]. However, whether autophagy-dependent cell death involved in 5-ALA-PDT against keloid remains unknown. Therefore, we first intend to confirm the molecular mechanisms involved in 5-ALA-PDT induced inhibitory effect on keloid.

It has been demonstrated that ROS generation can induce autophagy [10]. More importantly, SIRT1 and SIRT3 can regulate mROS homeostasis and autophagic flux [11,12]. Hence, we also focus on SIRT1-SIRT3 pathway in response to 5-ALA-PDT against keloid.

## 2. Materials and methods

### 2.1. Primary culture of fibroblasts

This study was approved by the ethics committee of Shanghai Jiao Tong University School of Medicine. Six keloid tissue specimens were kindly provided by patients underwent surgery. The method for isolation and culture of keloid–derived fibroblasts was performed as described previously with minor modifications. Briefly, keloid samples were dissected into 1-mm-long pieces, and then subjected to 0.25% collagenase type I (Sigma-Aldrich) for 6 h before complete dissociation by trituration with a narrowed Pasteur pipette. The filtered cells were collected and cultured in Dulbecco's Modified Eagle Medium (Invitrogen) containing 10% fetal bovine serum (Hyclone Laboratories, Inc., Logan, Utah) at 37 °C in a humidified chamber with 5% carbon dioxide and 21% oxygen. The medium was changed every 72 h. Cells from passages 3 through 6 were used in the following experiments.

#### 2.1.1. 5-ALA–derived protoporphyrin IX and photodynamic therapy treatment

5-ALA was purchased from Sigma-Aldrich (St. Louis, Mo.). When Keloid–derived fibroblasts reached 80–90% confluence, the medium was replaced with a serum-free medium with various concentrations of 5-ALA for 6 h in the dark. Intracellular accumulation of 5- ALA–derived protoporphyrin IX was observed by fluorescence microscopy (Leica DMI3000; Leica Microsystems, Wetzlar, Germany). Keloid–derived fibroblasts were then washed with PBS and irradiated by 630-nm light using a diode laser (Photoelectric Medical Instrument Factory, Guilin, China) for 0.5 h. Finally, cells were incubated with fresh medium for another 16 h.

### 2.2. Cytotoxicity assay

The cytotoxicity assay was determined with the Cell Counting Kit 8 (CCK-8) assay (CK04; Dojindo, Kumamoto, Japan). In short, keloid–derived fibroblasts were seeded in 96-well culture plates ($5 \times 10^3$ cells/well) and allowed to incubate for 24 h. Then cells were cultured for another 12 h after treated with 5-ALA and/or photodynamic therapy. The CCK-8 assay reagent (10 μl) was added to each well, and the plates were incubated at 37 °C for 4 h. Absorbance was measured at 450 nm using a Multiskan Spectrum reader (Thermo Scientific, Waltham, MA, USA).

### 2.3. Apoptosis detection

Cell apoptosis was determined by terminal deoxynucleotidyl transferase (TdT) nick-end labeling (TUNEL) assay. Keloid-derived fribroblasts apoptosis was further confirmed by flow cytometric analyses using an annexin V–fluorescein isothiocyanate/propidium iodide double staining kit (Becton, Dickinson & Co., Franklin Lakes, N.J.). Cell populations were stained with a mixture of fluorescein isothiocyanate–conjugated annexin V binding to membrane phosphatidylserine and propidium iodide binding to DNA as described previously. Briefly, cells were harvested, washed twice in ice cold phosphate-buffered saline, and stained by 5 μl of annexinV–fluorescein isothiocyanate and 5 μl of propidium iodide for 15 min at room temperature. Subsequently, quantitative analysis of apoptosis was performed using a flow cytometer (Becton Dickinson).

### 2.4. Electron microscopy

To morphologically observe the induction of autophagy in 5-ALA-PDT treated keloid–derived fibroblasts, electron microscopy was used. Cells were washed thrice with phosphate-buffered saline and fixed with ice-cold glutaraldehyde for 0.5 h at 4 °C. Then fixed in 1% osmium tetroxide for 0.5 h at 4 °C and embedded in LX 122 before being cut and stained with uranyl acetate/lead citrate. At last, observed using a Hitachi-7500 electron microscope (Hitachi Instrument, Tokyo, Japan).

### 2.5. Evaluation of autophagic cells

Cells were transfected with tandem fluorescent mRFP-GFP-LC3B (HanHeng, Shanghai, China) in a 60-mm cell culture dish for 4 h, according to the manufacturer's instructions, then the media were exchanged for fresh complete media, cultured for additional 44 h. Cells were treated with either control vehicle or 5-ALA-PDT 0.5 h, after 12 h, imaged using a Zeiss confocal laser scanning microscope. The number of GFP and RFP dots was determined by manual counting of fluorescence puncta.

### 2.6. Measurement of ROS

To assess mitochondrial-derived ROS, cells were incubated with culture medium containing 10 mM MitoSOX (Invitrogen, M36008) for 30 min. The fluorescence intensity was measured with an Infinite™ M200 Microplate Reader at an excitation wavelength of 492 nm and an emission wave length of 595 nm. Cellular fluorescence intensity is displayed as the fold change relative to the control.

### 2.7. Measurement of SOD2 enzyme activity

SOD2 enzymatic activity was performed using a SOD Assay Kit with WST-8 (Beyotime Company, S0103) according to the manufacturer's instructions. SOD enzyme activity includes SOD1 and SOD2 enzyme activity, so adding SOD1 inhibitor A and B to inhibit SOD1 activity. The absorption at 450 nm was measured using an InfiniteTM M200 Microplate Reader.

### 2.8. Protein immunoblotting analysis

Equivalent amounts of protein (30 μg per lane) were loaded and separated by 12% SDS-PAGE gels and transferred electrophoretically to PVDF membranes. Following protein transfer to PVDF membranes, the membranes were blocked and then incubated overnight at 4 °C with specific primary antibodies as follows: SIRT1, HIF-1α, SIRT3, p62, LC3, SOD2, TGF-β1, collagen-1, Smad-3 and β-actin were obtained from Cell Signaling Technology, Inc. (Beverly, Mass.). The bands of proteins were visualized using the ECL Plus system (GE Healthcare, Little Chalfont, United Kingdom). Image J (Scion Corporation) was used to quantify the optical density of each band.

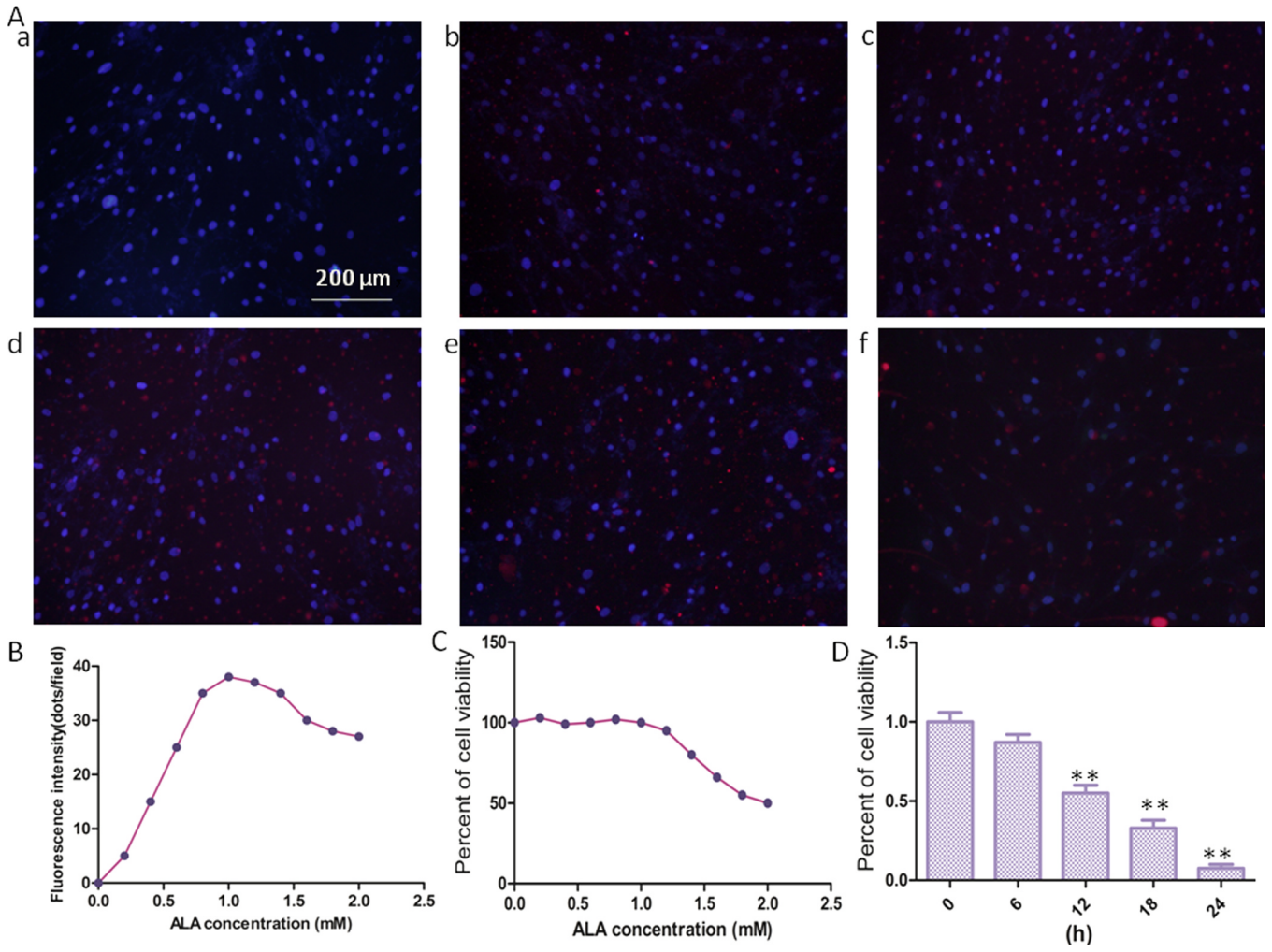


**Fig. 1.** Accumulation of 5-ALA–derived protoporphyrin IX and the effects of 5-ALA alone or 5-ALA-PDT on cell viability of keloid–derived fibroblasts. (A) Representative images of protoporphyrin IX accumulation (red) and nucleus location (blue) detected by fluorescence microscopy (original magnification, × 200), (a) 0 mM/ml; (b) 0.4 mM/ml; (c) 0.8 mM/ml; (d) 1.2 mM/ml; (e) 1.6 mM/ml; (f) 2.0 Mm/ml. (B) Quantification of fluorescence protoporphyrin IX fluorescence was analyzed by LAS AF software (Leica). Cell viability measured by CCK-8 assay in the present of 5-ALA(C),or in the present of 5-ALA-PDT and expressed as means ± SEM (*$p < 0.05$ and **$p < 0.01$ compared with control group).

### *2.9. Real-time polymerase chain reaction*

Total RNA was extracted from collected cells with Trizol reagent (Takara Bio Inc., Shiga, Japan) according to manufacturer's instructions. The quantity of extracted RNA was detected using the Nanodrop 2000 spectrophotometer (NanoDrop Products, Wilmington, Del.). High-quality RNA was reverse transcribed to cDNA using a Prime Script RT reagent Kit (Takara). The SIRT3 probes were (50-GACATTCGGGCTGA CGTGAT-30) and (50-ACCACATGCAGCAAGAACC TC-30), the GAPDH probes were (50- TGACAACAGCCTCAAGAT-30) and (50-GAGTCCTTC CACGATACC-30). Polymerase chain reaction amplification was carried out using SYBR Premix Ex Taq (Takara). Amplification and quantitative polymerase chain reaction measurements were using the Applied Biosystems 7500 Fast Real-Time PCR System (Applied Biosystems, Foster City, Calif.). Relative quantifications and calculations were performed using the comparative threshold cycle method ($2^{-\Delta\Delta CT}$).

### *2.10. Immunoprecipitation*

Cells were treated with 5-ALA and photodynamic therapy, then lysed with cell lysis buffer (Beyotime Company, P0013). Lysates were clarified by centrifugation at 12,000 g for 10 min and were used for immunoprecipitation. A total of 2 mg of antibody was incubated with 500–1000 mg of protein overnight at 4 ℃. Next, protein A beads (Beyotime Company, P2006) were added and the mixture was incubated overnight at 4 ℃. The beads were washed 3 times, then solubilized in 40 ml 3xSDS sample buffer (Cell Signaling Technology, 7722), and analyzed by western blotting.

### *2.11. Statistical analysis*

All values in this study were expressed as mean ± SEM from at least three independent experiments. Statistical analysis was performed using one-way analysis of variance followed by *t*-test to investigate whether the differences were significant between the mean values of different groups. Values of $p < 0.05$ were regarded as statistically significant. All statistical analyses were performed using GraphPad Prism-5 software.

## 3. Results

### *3.1. 5-ALA-PDT significantly reduces cell viability of keloid–derived fibroblasts*

The efficacy of photodynamic therapy, at least in part, depends on the intracellular photosensitizer accumulation, which has been well-

regarded as a prognostic factor of therapeutic outcomes in tumor tissues [13–15]. Protoporphyrin IX fluorescence was observed by fluorescence microscopy in keloid–derived fibroblasts incubated with 5-ALA concentrations ranging from 0 to 2.0 Mm/ml for 4 h. As shown in Fig. 1A and Fig. 1B, the intensity of protoporphyrin IX fluorescence enhanced with increased 5-ALA doses in the range between 0 and 1 mM/ml. However, protoporphyrin IX fluorescence declined when 5-ALA doses beyond 1 mM/ml, which mainly due to 5-ALA can induce cell death beyond 1 mM/ml. And CCK-8 assay (Fig. 1C) displayed that 5-ALA has no effect on cell viability ranging from 0 to 1 Mm/ml, but high concentrations of 5-ALA can induce cell death.

According to preliminary 5-ALA fluorescence assay and a sizable body of literature,12, 24–26 we identified the following optimizing parameters: 5-ALA doses (1 Mm/ml), and a laser power density of 2 J/cm2. Therefore, all subsequent experiments were performed under these conditions. The exposure time is half an hour, and then cultured for subsequent experiments. Fig. 1D shown that 5-ALA-PDT significantly reduces cell viability of keloid–derived fibroblasts, after exposure, cell viability gradually decreased over time.

### 3.2. 5-ALA-PDT enhanced autophagy of keloid–derived fibroblasts

Cells were treated with 5-ALA-PDT for 0.5 h. Next, the cells were washed twice and cultured for another 12 h. Electron microscopy was used to morphologically observe the induction of autophagy in keloid–derived fibroblasts. As shown in Fig. 2A, both autophagosome and autolysosome accumulate markedly in cells after treatment with 5-ALA-PDT. AS the same time, western blot shown that LC3-II/β-actin level was significantly increased with the increasing of time after 5-ALA-PDT exposure and p62 protein level was decreased, indicated that autophagy was promoted by 5-ALA-PDT (Fig. 2B). To further detect autophagic flux, cells were transfected with tandem fluorescent mRFP-GFP-LC3B. Found that autophagosomes and autolysosomes (Fig. 2C) in the cells treated with 5-ALA-PDT increased markedly.

### 3.3. 5-ALA-PDT induced death of keloid–derived fibroblasts may not through apoptosis pathway

5-ALA-PDT can obviously induce death of keloid–derived fibroblasts, However, the mechanism remains to be elucidated. Although many studies [16,17] have reported that apoptosis plays a key role in other cells treated with PDT, TUNEL assay (Fig. 3A) shown there was no difference between the 5-ALA-PDT group and the control group. To further investigate whether apoptosis plays a key role in keloid–derived fibroblasts treated with 5-ALA-PDT, flow cytometric analyses (Fig. 3B) was performed. Compared with control group, there was no difference

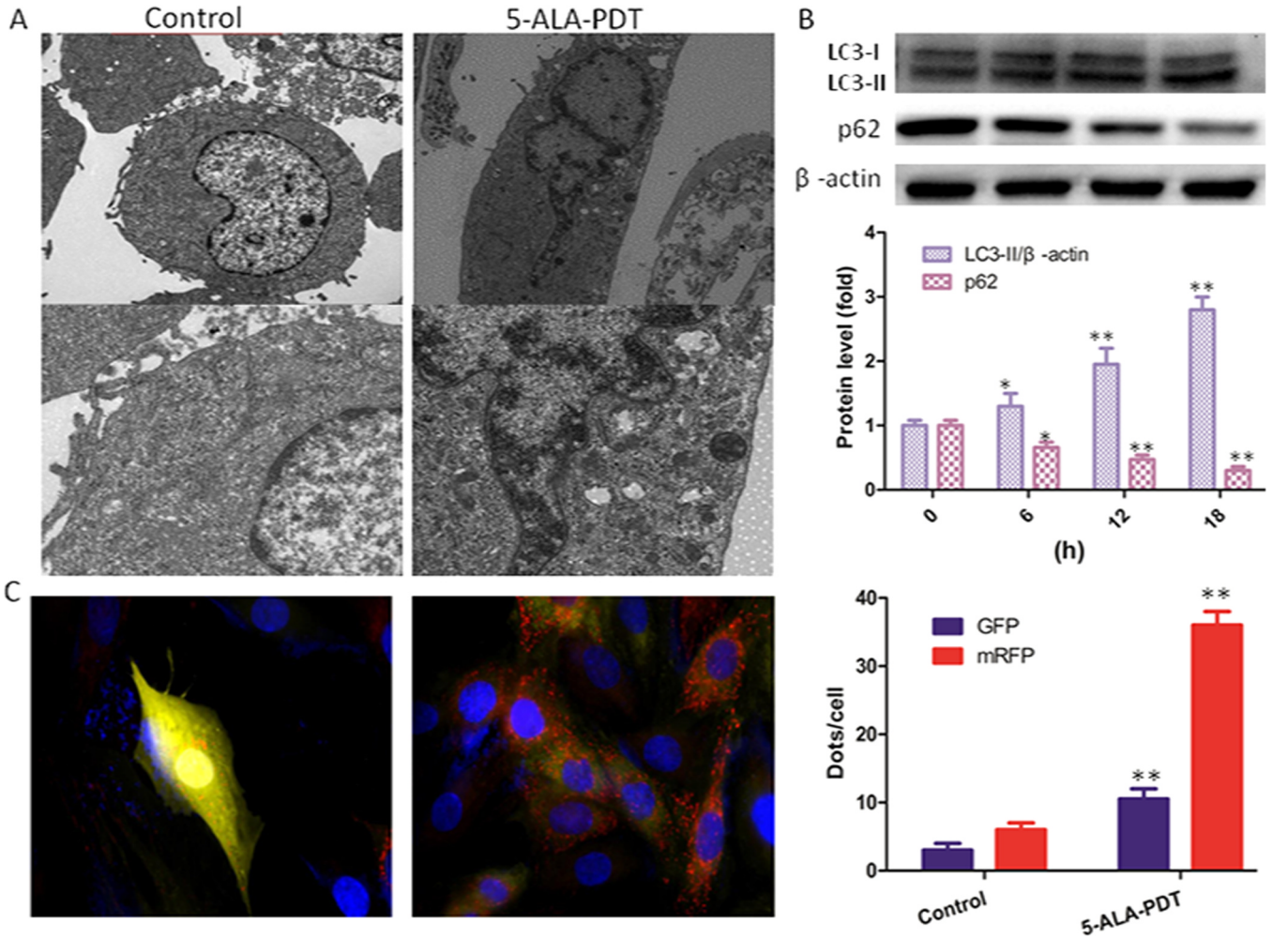


**Fig. 2.** 5-ALA-PDT promoted autophagy in keloid–derived fibroblasts. (A) Electron microscopy revealed an increased number of autophagic vacuoles with exposure to 5-ALA-PDT for 12 h compared with control group. (B) Immunoblot and quantification analysis of LC3 and p62 performed after cells were treated with 5-ALA-PDT at different time (0, 6, 12, 18 h). β-actin used as an internal standard for protein loading. (C) The formation of autophagosomes and autolysosomes were explored through transfecting with tandem fluorescent mRFP-GFP-LC3B. using confocal microscopy and was quantified. The values are presented as the means ± SEM, *$p < 0.05$, **$p < 0.01$ versus control group. All experiments were repeated three times.

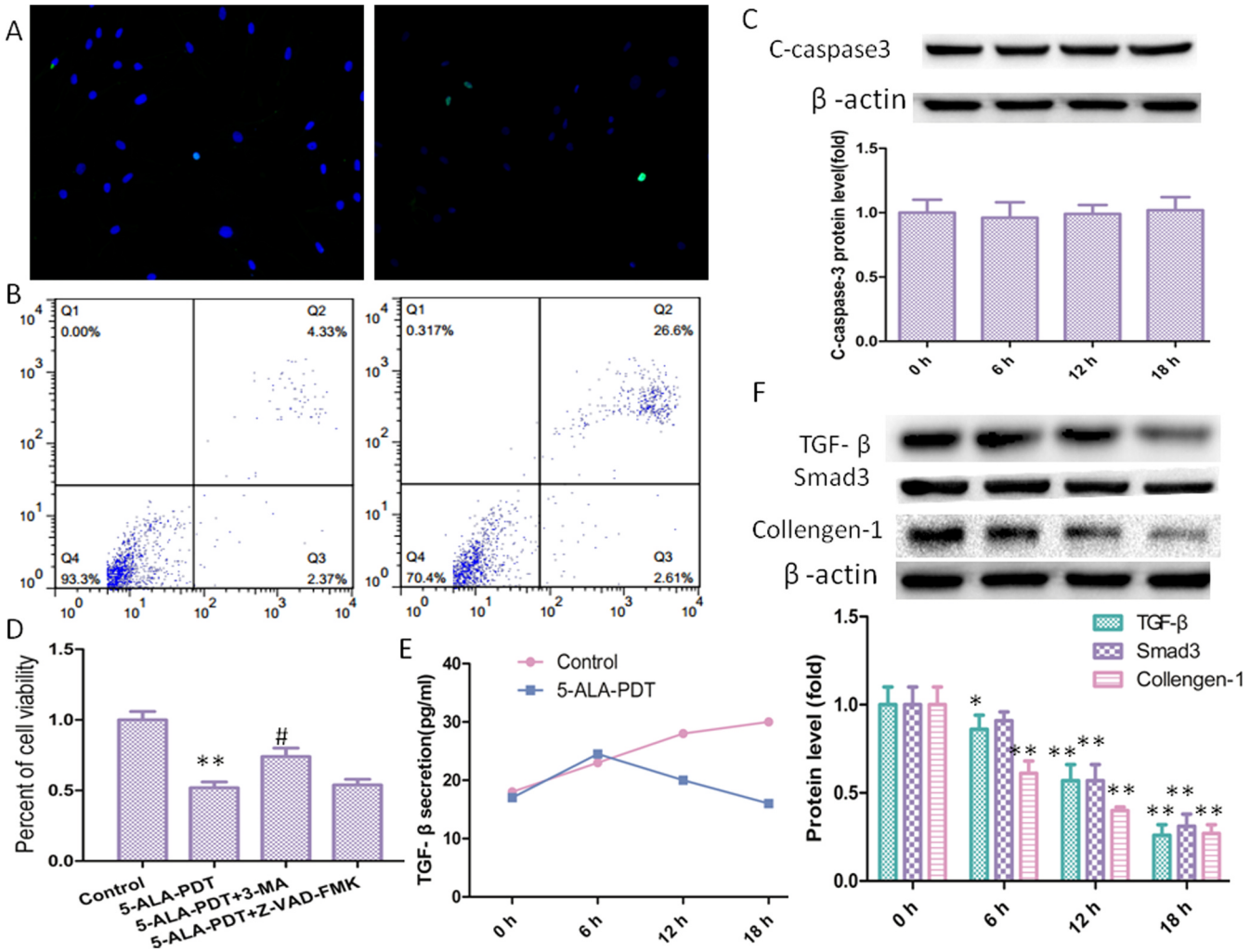


**Fig. 3.** 5-ALA-PDT induced death of keloid–derived fibroblasts may through autophagy pathway. (A) 5-ALA-PDT did not induce apoptosis in keloid–derived fibroblasts demonstrated by TNNEL assay. (B) Flow cytometric analyses for 5-ALA-PDT induced apoptosis in keloid–derived fibroblasts. (C) Western blot and quantification analysis of C-caspase 3. (D) 3-MA (autophagy inhibitor ) significantly inhibited 5-ALA-PDT induced death of keloid–derived fibroblasts, but Z-VAD-FMK (apoptotic inhibitor) did not. (E) TGF-β secretion was measured by ELISA assay. (F) TGF-β1, Smad3 and Collagen-1 were detected by western blot. The values are presented as the means ± SEM, *$p < 0.05$, **$p < 0.01$ compared with control group, $^{\#}p < 0.05$ compared with 5-ALA-PDT group. All experiments were repeated three times.

in early apoptosis in 5-ALA-PDT group displaying that 5-ALA-PDT induced death of keloid–derived fibroblasts may not through apoptosis pathway. Consistent with the above results, western blot shown that C-caspase-3 was not increased after 5-ALA-PDT exposure.

Autophagy, a degradation mechanism that attenuates aging of cells through degrading long-lived proteins, pathogens, damaged DNA elements, and damaged organelles, activated especially during metabolic stress conditions. However, there is already growing evidence that excess autophagy may induce mitochondrial loss, cellular energy depletion and cell death [8,9]. In order to further explore whether apoptosis or autophagy is involved in 5-ALA-PDT induced death of keloid–derived fibroblasts, Z-VAD-FMK (apoptosis inhibitor) and 3-MA (autophagy inhibitor) were used, found that 3-MA obviously inhibited 5-ALA-PDT induced cell death, but Z-VAD-FMK did not (Fig. 3C). These results indicated that 5-ALA-PDT induced death of keloid–derived fibroblasts may through autophagic cell death. The overexpressed TGF-β/Smad-3 signaling is another well-regarded mechanism underlying keloid, hence, ELISA assay (Fig. 3D) was used to detect TGF-β secretion displaying that 5-ALA-PDT can significantly decrease TGF-β secretion in keloid–derived fibroblasts. And in line with the change trend for TGF-β secretion, the TGF-β, Smad-3 and collagen-1 (Fig. 3E) protein level was also downregulated.

### 3.4. ROS mediates 5-ALA-PDT -induced autophagy

5-ALA, a precursor of heme biosynthesis, that located in mitochondria, could be enzymatically converted into protoporphyrin IX, which in turn interacts with tissue-penetrating light to produce ROS that ultimately induced cell destruction. MitoSOX-based measurements revealed that mROS levels were significantly increased, moreover, mitochondrial-derived ROS levels gradually increased over time (Fig. 4A). Then, cells were preincubated with 10 mM Mito-TEMPO before and after the treatment of 5-ALA-PDT. The mitochondrial antioxidant Mito-TEMPO (mitochondrial-targeted SOD mimetic) decreased mROS obviously (Fig. 4B). In many studies, mROS have been implicated in autophagy [18–20]. Consistent with these studied, 5-ALA-PDT increased LC3-II/β-actin protein level, which was significantly attenuated after treatment with Mito-TEMPO (Fig. 4C).

Hypoxia-inducible factor-1 alpha (HIF-1α) is a transcription factor that activates the transcription of genes and is responsible for progression of cell survival and proliferation. The accumulation of HIF-1α can be stimulated via hypoxia-independent mechanisms. Many studies [21,22] have shown that HIF-1α can enhance autophagy, therefore, we speculate that ROS may enhance cell autophagy through HIF-1α. Western blot was used to detect HIF-1α, found that 5-ALA-PDT

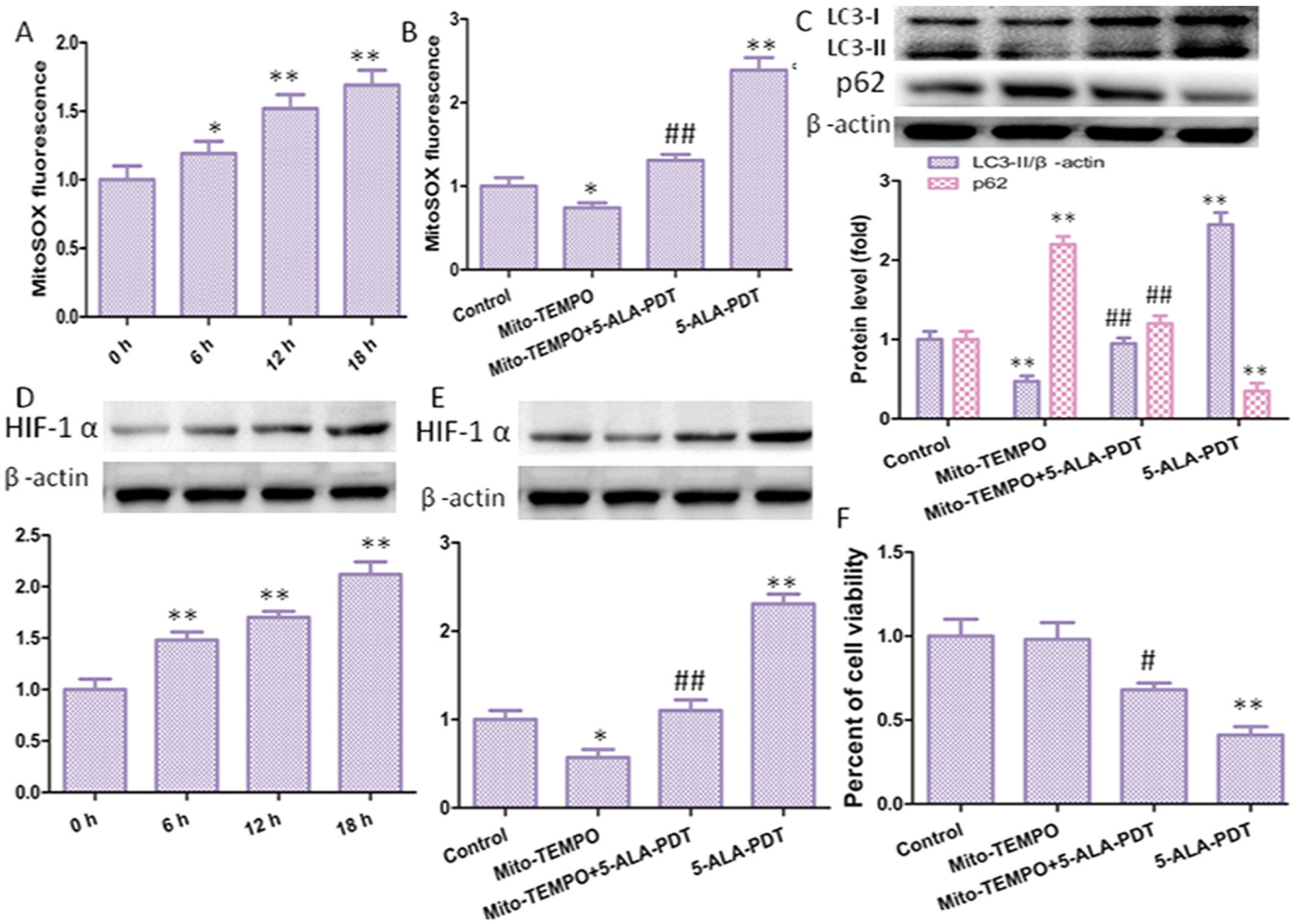


**Fig. 4.** mROS involved in 5-ALA-PDT induced autophagy. (A) Quantification of mROS level using a fluorescence spectrometer after cells were treated with 5-ALA-PDT at different time (0, 6 12, 18 h). Cells were preincubated with Mito-TEMPO and then treated with 5-ALA-PDT for 12 h. Then mROS level (B) and LC3 protein level (C) and were determined. (D) 5-ALA-PDT promoted upregulation of HIF-1α protein level, and Mito-TEMPO decreased HIF-1α protein level (E), meanwhile, Mito-TEMPO inhibited 5-ALA-PDT induced death of keloid-derived fibroblasts (F). The values are presented as the means ± SEM, *p < 0.05, **p < 0.01 versus control group, $^{\#}$p < 0.05, $^{\#\#}$p < 0.01 versus 5-ALA-PDT group. All experiments were repeated three times.

increased HIF-1α protein level (Fig. 4D), and Mito-TEMPO significantly reversed this effect (Fig. 4E). Moreover, 5-ALA-PDT decreased cell viability that significantly attenuated after treatment with Mito-TEMPO (Fig. 4F).

### 3.5. 5-ALA-PDT increases SIRT3 expression and activity of SOD2

SOD2, the primary mitochondrial oxidative scavenger, plays a key role in the regulation of ROS [23]. The effects of 5-ALA-PDT induced mROS production on SOD2 expression were investigated. Interestingly, 5-ALA-PDT significantly increased SIRT3 protein level and SOD2 activity in a time-dependent manner without changing SOD2 protein level (Fig. 5A). SIRT3 is a soluble protein located in the mitochondrial matrix, which exhibits $NAD^+$-dependent deacetylase activity involved in mitochondrial energy production and limits the accumulation of mROS. Deacetylation of SOD2 by SIRT3 regulates SOD2 enzymatic activity has been identified [24]. Then we explored SOD2 acetylation level with immunoprecipitation and subsequent western blot using an anti-acetyllysine antibody. Found that 5-ALA-PDT significantly increased the acetylation levels of SOD2 compared with control group (Fig. 5B). In order to confirm deacetylation of SOD2 regulated by SIRT3, 3-TYP (SIRT3 inhibitor) was used. Found that inhibition of SIRT3 by 3-TYP significantly increased the level of SOD2 acetylation level compared with control group or 5-ALA-PDT group (Fig. 5C). Next, SOD2 activity was measured and found that 5-ALA-PDT significantly increased SOD2 activity in a time-dependent manner. Consistent with above results, inhibition of SIRT3 by 3-TYP significantly increased the level of mROS level compared with control group or 5-ALA-PDT group. Hence, the activation of SIRT3-SOD2 pathway compromised the efficacy of 5-ALA-PDT against keloid. RT-PCR assay (Fig. 5D) shown that 5-ALA-PDT increased SIRT3 mRNA level.

### 3.6. SIRT1 is involved in up-regulation of SIRT3-SOD2 pathway

SIRT1 and SIRT3 are two well-characterized members of the silent information regulator 2 (Sir2) family of proteins, but the interaction between these two sirtuins has not been fully determined. In this study, found that SIRT1 may inhibit the activity of SIRT3-SOD2 pathway, 5-ALA-PDT induced SIRT1 protein degradation in time-dependent way (Fig. 6A). First, cells were treated with EX527(SIRT1 inhibitor) or SRT1720 (SIRT1 activator), and EX527 increased SIRT3 protein level, however, SRT1720 displayed the opposite effect in the present or absence of 5-ALA-PDT (Fig., 6B). Next, the effect of SIRT1 on autophagy was performed, we found that SRT1720 increased LC3-II protein level and EX527 decreased LC3-II level with or without 5-ALA-PDT (Fig. 6C). As the same time, SRT1720 increased mROS level, and EX527 decreased mROS level, in the present of 5-ALA-PDT, which in line with our expectations (Fig. 6D). We also explored the effect of SIRT1 on cell

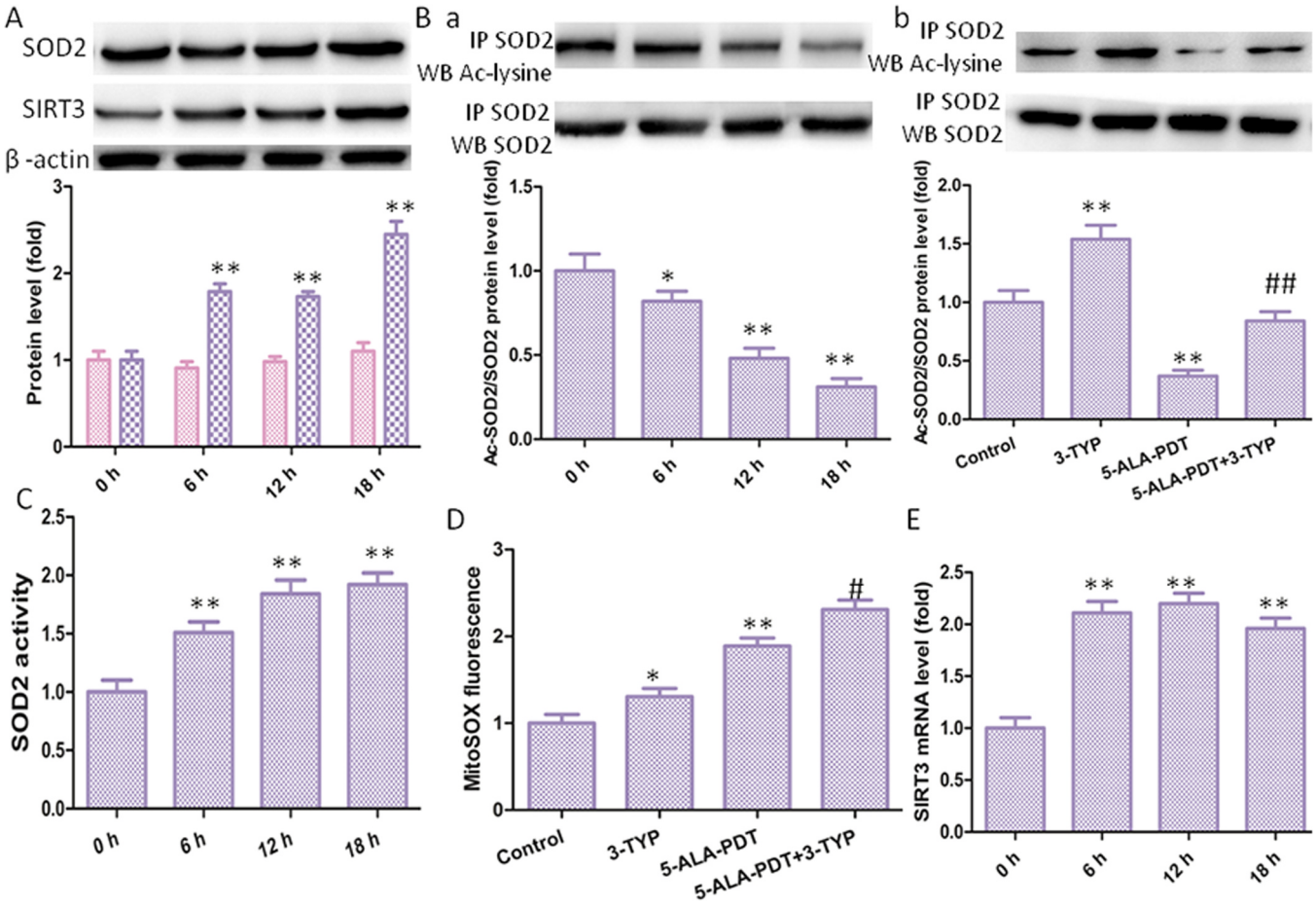


**Fig. 5.** 5-ALA-PDT exposure increased SIRT3-SOD2 pathway in keloid-derived fibroblasts. (A) The protein levels of SIRT3 and SOD2 were evaluated by western blotting. (B) Acetylation of SOD2 after 5-ALA-PDT exposure was determined by immunoprecipitation with an anti-SOD2 antibody, followed by immunoblot analysis of acetylated-lysine. (C) Acetylation of SOD2 after treatment with 3-TYP. (D) SOD2 activity in keloid-derived fibroblasts. (E) mROS level in keloid-derived fibroblasts after treatment with 3-TYP. (F) SIRT3 mRNA level after 5-ALA-PDT exposure. The values are presented as the means ± SEM, $^{*}p < 0.05$, $^{**}p < 0.01$ versus untreated group, $^{\#}p < 0.05$, $^{\#\#}p < 0.01$ versus 5-ALA-PDT group. All experiments were repeated three times.

viability, found that EX527 significantly inhibited efficacy of 5-ALA-PDT against keloid- keloid–derived fibroblasts and SRT1720 induced the opposite effect in the present of 5-ALA-PDT (Fig. 6E).

## 4. Discussion

Although there are many forms of treatment for keloid, they exist some disadvantages such as low efficacy, side effects and high risk of palindromia. Hence, the search for safer and more effective therapies for keloid seems to be required urgently. PDT, an effective local treatment for malignant skin conditions and many other types of tumors with great spatiotemporal accuracy and minimal invasiveness, has been suggested as a promising treatment for keloid [25–27]. A growing number of studies have investigated the mechanisms involved in 5-ALA-PDT, but these findings almost highlight the role of apoptosis in 5-ALA-PDT [16,17,28]. In order to explore whether apoptosis involved in 5-ALA-PDT against keloid, keloid-derived fibroblasts were incubated with Z-VAK-FMK (apoptotic inhibitor) after 5-ALA-PDT treatment. Unexpectedly, Z-VAK-FMK did not inhibit death of keloid-derived fibroblasts induced by 5-ALA-PDT. Therefore, 5-ALA-PDT against keloid that is through other pathway, but not via inducing cells apoptosis.

Autophagy degrades long-lived proteins, pathogens, damaged DNA elements, and damaged organelles, activated especially during metabolic stress conditions [29]. Growing evidences have demonstrated that the basal level of autophagy is essential for the function and survival of cells [30,31]. Autophagy may contribute to cell survival by removing cells damaged by toxic metabolites and intracellular pathogens [32]. However, excessive autophagy may also lead to mitochondrial loss, cellular energy depletion and cell death through excessive self-digestion and degradation of essential cellular constituents [8,9,33]. We found that autophagy level increased after 5-ALA-PDT, and 3-MA, an autophagy inhibitor, significantly inhibited cells death induced by 5-ALA-PDT. This only confirms previously suspicion that autophagy may be the primary contributing factor underlying keloid-derived fibroblasts death induced by 5-ALA-PDT. 5-ALA, a precursor of heme biosynthesis, when located in mitochondria, could be enzymatically converted into protoporphyrin IX, an endogenous photosensitizer, which in turn interacts with tissue-penetrating light to produce ROS [5]. ROS can damage lipid, DNA, RNA, and proteins, which, in theory, contributes to the physiology of aging. The molecular mechanism underlying autophagy has been extensively investigated in recent years. The mitochondrial antioxidant Mito-TEMPO (mitochondrial-targeted SOD mimetic) enhanced SOD2 activity but not SOD2 levels, significantly suppressed the 5-ALA-PDT-mediated increase in autophagy level, and consistent with many studies revealed that ROS can induce autophagy [34–36].

Mitochondria play a central role in the production of reactive oxygen species as byproducts of metabolism and energy production. SOD2, the primary mitochondrial oxidative scavenger, plays a key role in the regulation of mROS, and SOD2 activity is tightly related with acetylation at its lysine residues [24]. SIRT3 (sirtuin 3), a primary mitochondrial acetyl-lysine deacetylase, regulates various proteins deacetylase to control mitochondrial function and mROS homeostasis

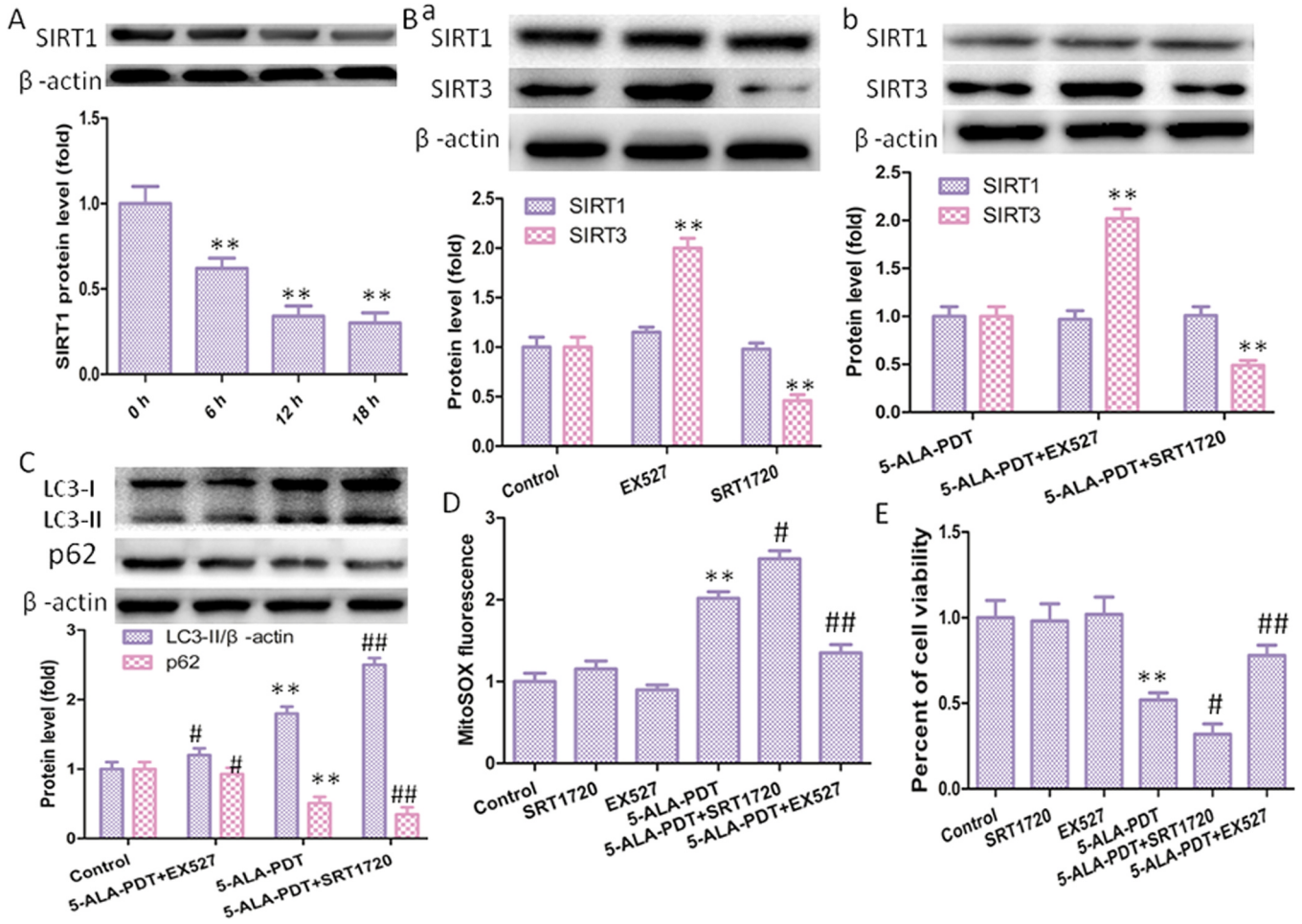


**Fig. 6.** SIRT1 involved in upregulation of SIRT3 protein level. (A) SIRT1 protein level measured by western blotting after 5-ALA-PDT exposure. (B) SIRT1 regulated SIRT3 protein level in the absence (Ba) or present (Bc) of 5-ALA-PDT detected by western blotting. (C) SIRT1 promoted autophagy in keloid-derived fibroblasts in the present of 5-ALA-PDT, as explored by western blot. (D) mROS level in keloid-derived fibroblasts treated with EX527 or SRT1720. (E) SIRT1 regulated cell viability in the present of 5-ALA-PDT. The values are presented as the means ± SEM, *$p < 0.05$, **$p < 0.01$ versus control group, $^{\#}p < 0.05$, $^{\#\#}p < 0.01$ versus 5-ALA-PDT group. All experiments were repeated three times.

[37]. SIRT3 primarily modulates mROS clearance via altering acetylation of SOD2. More importantly, SIRT3 directly binds and deacetylates SOD2, which increases SOD2 activity and plays a key role in mROS homeostasis and autophagic flux [11,12].

SIRT1, the most widely studied sirtuins, has been extensively documented in response to stress conditions [38,39]. But the precise role remains controversial. For example, in several studies SIRT1 has been reported to protect against oxidative stress-induced apoptosis, mainly by modulating the activity of FOXOs or p53 [32,40]. SIRT1 can also promote cell death in response to stressful condition. In particular, it has been reported that SIRT1 negatively regulated cell growth and survival of pancreatic cancer cells [38]. These studies indicated SIRT1 presented different roles might be attributed to different experimental setting conditions and tissue or cellular model.

In the present work we showed that SIRT1 exacerbated cell death in response to 5-ALA-PDT, however, 5-ALA-PDT can induce SIRT1 protein downregulation, which compromised the efficacy of 5-ALA-PDT against keloid-derived fibroblasts through downregulation of SIRT3-SOD2-mROS dependent autophagy pathway.

## Acknowledgments

This work was supported by National Natural Science Foundation Youth Science Fund Project (No. 81701949), and the Research Project of Shanghai Municipal Commission of Health and Family Planning (No. 201540374).

## Conflict of interest

The authors state no conflict of interest.

## References

[1] S. Kim, et al., Annexin A2 participates in human skin keloid formation by inhibiting fibroblast proliferation, Arch. Dermatol. Res. 306 (4) (2014) 347–357.
[2] Z. Hu, et al., TIEG1 represses Smad7-mediated activation of TGF-β1/smad signaling in keloid pathogenesis, J. Investig. Dermatol. 137 (5) (2017) 1051–1059.
[3] T. Gu, et al., Upconversion composite nanoparticles for tumor hypoxia modulation and enhanced NIR-triggered photodynamic therapy, ACS Appl. Mater. Interfaces (2018).
[4] M. Chang, et al., Potential molecular mechanisms involved in 5-aminolevulinic acid-based photodynamic therapy against human hypertrophic scars, Plast. Reconstr. Surg. 136 (4) (2015) 715–727.
[5] M. Jarvi, et al., Singlet oxygen luminescence dosimetry (SOLD) for photodynamic therapy: current status, challenges and future prospects, Photochem. Photobiol. 82 (5) (2006) 1198–1210.
[6] N. Bruscino, T. Lotti, R. Rossi, Photodynamic therapy for a hypertrophic scarring: a promising choice, Photodermatol. Photoimmunol. Photomed. 27 (6) (2011) 334–335.
[7] X. Li, et al., Apoptotic cell death induced by 5-aminolaevulinic acid-mediated photodynamic therapy of hypertrophic scar-derived fibroblasts, J. Dermatol. Treat. 25 (5) (2014) 428–433.

[8] H. Pi, et al., SIRT3-SOD2-mROS-dependent autophagy in cadmium-induced hepatotoxicity and salvage by melatonin, Autophagy 11 (7) (2015) 1037–1051.
[9] H. Pi, et al., Dynamin 1-like-dependent mitochondrial fission initiates overactive mitophagy in the hepatotoxicity of cadmium, Autophagy 9 (11) (2013) 1780–1800.
[10] E. Essick, F. Sam, Oxidative stress and autophagy in cardiac disease, neurological disorders, aging and cancer, Oxid. Med. Cell. Longev. 3 (3) (2010) 168–177.
[11] X. Qiu, et al., Calorie restriction reduces oxidative stress by SIRT3-mediated SOD2 activation, Cell Metab. 12 (6) (2010) 662–667.
[12] Q. Liang, et al., Bioenergetic and autophagic control by Sirt3 in response to nutrient deprivation in mouse embryonic fibroblasts, Biochem. J. 454 (2) (2013) 249–257.
[13] H. Xu, et al., Anti-proliferative effect of Juglone from Juglans mandshurica Maxim on human leukemia cell HL-60 by inducing apoptosis through the mitochondria-dependent pathway, Eur. J. Pharmacol. 645 (1–3) (2010) 14–22.
[14] Z. Luksiene, P. de Witte, Hypericin as novel and promising photodynamic therapy tool: studies on intracellular accumulation capacity and growth inhibition efficiency, Medicina 39 (7) (2003) 677–682.
[15] R. Ritz, et al., In vitro comparison of hypericin and 5-aminolevulinic acid-derived protoporphyrin IX for photodynamic inactivation of medulloblastoma cells, PLoS One 7 (12) (2012) e51974.
[16] H. Zhang, et al., High-voltage pulsed electric field plus photodynamic therapy kills breast cancer cells by triggering apoptosis, Am. J. Transl. Res. 10 (2) (2018) 334–351.
[17] Q. Huang, et al., Apoptosis and autophagy induced by pyropheophorbide-α methyl ester-mediated photodynamic therapy in human osteosarcoma MG-63 cells, Apoptosis 21 (6) (2016) 749–760.
[18] L. Sena, N. Chandel, Physiological roles of mitochondrial reactive oxygen species, Mol. Cell 48 (2) (2012) 158–167.
[19] J. Kim, et al., Mitochondrial ROS-derived PTEN oxidation activates PI3K pathway for mTOR-induced myogenic autophagy, Cell Death Differ. (2018).
[20] M. Sharma, R. Pandey, D. Saluja, ROS is the major player in regulating altered autophagy and lifespan in sin-3 mutants of C. elegans, Autophagy 14 (7) (2018) 1239–1255.
[21] Y. Wu, et al., Neuroprotection of deferoxamine on rotenone-induced injury via accumulation of HIF-1 alpha and induction of autophagy in SH-SY5Y cells, Neurochem. Int. 57 (3) (2010) 198–205.
[22] I. Papandreou, et al., Hypoxia signals autophagy in tumor cells via AMPK activity, independent of HIF-1, BNIP3, and BNIP3L, Cell Death Differ. 15 (10) (2008) 1572–1581.
[23] R. Tao, et al., Regulation of MnSOD enzymatic activity by Sirt3 connects the mitochondrial acetylome signaling networks to aging and carcinogenesis, Antioxid. Redox Signal. 20 (10) (2014) 1646–1654.
[24] R. Tao, et al., Sirt3-mediated deacetylation of evolutionarily conserved lysine 122 regulates MnSOD activity in response to stress, Mol. Cell 40 (6) (2010) 893–904.
[25] S. Karrer, et al., Influence of 5-aminolevulinic acid and red light on collagen metabolism of human dermal fibroblasts, J. Investig. Dermatol. 120 (2) (2003) 325–331.
[26] X. Wen, Y. Li, M. Hamblin, Photodynamic therapy in dermatology beyond non-melanoma cancer: an update, Photodiagn. Photodyn. Ther. 19 (2017) 140–152.
[27] S. Karrer, et al., Keratinocyte-derived cytokines after photodynamic therapy and their paracrine induction of matrix metalloproteinases in fibroblasts, Br. J. Dermatol. 151 (4) (2004) 776–783.
[28] A. Mamalis, et al., Temperature-dependent impact of thermal aminolaevulinic acid photodynamic therapy on apoptosis and reactive oxygen species generation in human dermal fibroblasts, Br. J. Dermatol. 175 (3) (2016) 512–519.
[29] D. Klionsky, et al., Guidelines for the use and interpretation of assays for monitoring autophagy (3rd edition), Autophagy 12 (1) (2016) 1–222.
[30] Y. Dong, et al., Involvement of autophagy induction in penta-1,2,3,4,6-O-galloyl-β-D-glucose-induced senescence-like growth arrest in human cancer cells, Autophagy 10 (2) (2014) 296–310.
[31] C. Zhao, et al., Autophagy-dependent EIF2AK3 activation compromises ursolic acid-induced apoptosis through upregulation of MCL1 in MCF-7 human breast cancer cells, Autophagy 9 (2) (2013) 196–207.
[32] T. Liu, et al., SIRT1 reverses senescence via enhancing autophagy and attenuates oxidative stress-induced apoptosis through promoting p53 degradation, Int. J. Biol. Macromol. 117 (2018) 225–234.
[33] Y. Liu, B. Levine, Autosis and autophagic cell death: the dark side of autophagy, Cell Death Differ. 22 (3) (2015) 367–376.
[34] K. Lee, et al., MYC and MCL1 cooperatively promote chemotherapy-resistant breast cancer stem cells via regulation of mitochondrial oxidative phosphorylation, Cell Metab. 26 (4) (2017) (p. 633-647.e7).
[35] M. Liu, et al., ROS-Autophagy pathway mediates monocytes-human umbilical vein endothelial cells adhesion induced by apelin-13, J. Cell. Physiol. (2018).
[36] H. Wang, et al., Chitosan nanoparticles triggered the induction of ROS-mediated cytoprotective autophagy in cancer cells, Artif. Cells Nanomed. Biotechnol. (2018) 1–9.
[37] A. Bause, M. Haigis, SIRT3 regulation of mitochondrial oxidative stress, Exp. Gerontol. 48 (7) (2013) 634–639.
[38] C. Chini, et al., SIRT1-activating compounds (STAC) negatively regulate pancreatic cancer cell growth and viability through a SIRT1 Lysosomal-dependent pathway, Clin. Cancer Res. 22 (10) (2016) 2496–2507.
[39] A. Herskovits, L. Guarente, SIRT1 in neurodevelopment and brain senescence, Neuron 81 (3) (2014) 471–483.
[40] Y. Wang, et al., SIRT1 Protects against oxidative stress-induced endothelial progenitor cells apoptosis by inhibiting FOXO3a via FOXO3a ubiquitination and degradation, J. Cell. Physiol. 230 (9) (2015) 2098–2107.